SECOND EUROPEAN CONFERENCE ON EARTHQUAKE ENGINEERING AND SEISMOLOGY, ISTANBUL AUG. 25-29, 2014

AUTO-PARAMETRIC MULTI-MODAL VIBRATION OF A CONTINUOUS SLENDER STRUCTURE DUE TO SEISMIC EXCITATION

Jiří NÁPRSTEK and Cyril FISCHER[1]

ABSTRACT

Non-linear dynamic effects are the most dangerous processes endangering structures during a seismic attack. Among them, auto-parametric non-linear vibration in state of post-critical auto-parametric resonance can lead to collapse particularly in case of high slender systems or large dynamically sensitive structures. The main cause of these effects is a strong vertical component of an earthquake excitation in epicentre area. In sub-critical linear regime vertical and horizontal response components are independent and therefore no horizontal response component is observed in such case. If the amplitude of a vertical excitation in a structure foundation exceeds a certain limit, a vertical response component loses dynamic stability; dominant horizontal response component arises and can lead to failure of the structure.

INTRODUCTION

The various non-linear dynamic effects are dangerous processes endangering structures during a seismic shock. The non-linear auto-parametric resonance, see Tondl et. al. (2000), Hatwal et al. (1983) or Bajaj et al. (1994), can lead to collapse particularly in case of high slender systems or large dynamically sensitive structures. The main cause of these effects is a strong vertical component of an earthquake excitation in epicentre area. In sub-critical linear regime the vertical and horizontal response components are independent and, therefore, no horizontal response is observed. The semi-trivial solution, in which all but the vertical component are zero, gives a full image of the structure behaviour. If the frequency of a vertical excitation in a structure foundation finds in a certain interval and its amplitude exceeds a certain limit, the vertical response component loses dynamic stability and dominant horizontal response component is generated, e.g., Benettin et al. (1980), and can lead to failure of the structure. This post-critical regime (auto-parametric resonance) follows from the strong non-linear interaction between vertical and horizontal response components. Consequently, in such a case the widely used linear approach usually does not provide any interesting knowledge.

The purely vertical excitation of an existing structure, as assumed in the current work, is mostly an idealisation of a certain type of seismic ground motion. On the other hand, significance of the vertical seismic component is regularly mentioned in the literature in since late 1990s (e.g., Broderick and Elnashai (1995), Elnashai and Papazoglou (1996), for comprehensive review see Ambraseys and Douglas (2000)). The dominant vertical character of a seismic motion has been repeatedly reported (e.g., Carydis et al. (2012)) being caused due to local site conditions. Moreover, in reality the mild horizontal component could help to start up the auto-parametric resonance.

Many studies dealing with analytical, numerical as well as experimental aspects of auto-parametric systems and their applications are available. They are given mostly by Tondl and co-authors, see for

[1]Institute of Theoretical and Applied Mechanics ASCR, v.v.i. Prosecká 76, Prague, Czech Republic
naprstek@itam.cas.cz

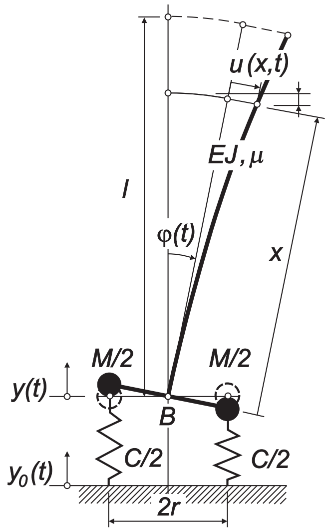

Figure 1: Outline of an auto-parametric model with a continuous vertical console

instance monograph (Tondl et. al., 2000). Certainly, many other authors contributed to this topic significantly, see, Bajaj et al. (1994), Hatwal et al. (1983), etc. The seismic type broadband random nonstationary excitation can be particularly dangerous and amplify these effects. From viewpoint of rational dynamics the problem is of the inverse pendulum type.

Auto-parametric systems similar to the presented one have been studied during recent years, see, e.g., authors papers Náprstek and Fischer (2008, 2009, 2011). The mathematical models used in these studies idealised the vertical structure as one concentrated mass related with the basement by a massless spring. However, the easily deformable tall structures are the most sensitive regarding effects of auto-parametric resonance. Therefore the structure itself is modelled as a console with continuously distributed stiffness and mass in order to respect the whole eigen-value spectrum, see (Náprstek and Fischer, 2012). Concerning subsoil conventional model including internal viscosity can be retained.

Outline of the paper is as follows: In the next section, the mathematical model of the structure is defined. The section 3 presents theoretical formulation of the semi-trivial solution and its stability limits; in the section 4 are commented the resonance properties of the model. The section that follow show numerical examples. Some conclusions are presented in the last section.

THEORETICAL MODEL

The differential system describing the model outlined in the Figure 1 can be deduced in the form of Lagrange equations for the kinetic and potential energies of the moving system. The formulation follows:

$$\begin{aligned} T(t) = {} & \frac{1}{2}M(\dot{y}^2(t)+r^2\dot{\varphi}^2(t))+ \\ & +\frac{1}{2}\mu\int_0^l [(\dot{\varphi}(t)x+\dot{u}(x,t))^2+\dot{y}^2(t)-2\dot{y}(t)(\dot{\varphi}(t)x+\dot{u}(x,t))\sin\varphi(t)]\mathrm{d}x, \end{aligned} \tag{1a}$$

$$\begin{aligned} U(t) = {} & Mg\cdot y(t)+\frac{1}{2}C((y(t)-y_0(t))^2+r^2\varphi^2(t))+ \\ & +\mu g\int_0^l [y(t)-x(1-\cos\varphi(t))-u(x,t)\sin\varphi(t)]\mathrm{d}x+\frac{1}{2}EI\int_0^l u''^2(x,t)\mathrm{d}x. \end{aligned} \tag{1b}$$

where:

$y = y(t), \zeta(t) = y(t)/l$ – vertical displacement of the B point and its non-dimensional form;
$y_0 = y_0(t), \zeta_0(t) = y_0(t)/l$ – kinematic excitation (seismic process) and non-dimensional form;
$\varphi = \varphi(t)$ – angular rotation of the system in the B point;
$u = u(x,t), \psi(\xi,t) = u(x,t)/l$ – bending deformation of the vertical console and non-dimensional form;
M – foundation effective mass;
C – subsoil effective stiffness;
$\mu, m = \mu l$ – console uniformly distributed and total mass;
EI – console bending stiffness (constant);
η_c, η_e – viscous damping parameters of the C, EI stiffness following Kelvin definition;
$r, l, \rho = r/l$ – geometric parameters;
$x, \xi = x/l$ – length coordinate along the console.

The material damping of the console is considered to be proportional. Therefore its deformation can be expressed in a form of a convergent series in dimensionless coordinates:

$$\psi(\xi,t) = \sum_{i=1}^{n} \alpha_i(t) \cdot \chi_i(\xi) \,, \qquad (\psi_i(x) = l \cdot \chi_i(\xi)), \tag{2}$$

where the basis functions $\chi_i(\xi)$ are eigen-functions (eigen-forms) of the differential equation:

$$\chi_i^{\text{iv}}(\xi) + \lambda_i \chi_i(\xi) \; = \; 0, \quad (\lambda_i/l)^4 = \mu \omega_i^2 / EI \tag{3}$$

Boundary conditions are valid for a console beam: $\chi_i(0) = 0,\ \chi_i'(0) = 0,\ \chi_i''(1) = 0,\ \chi_i'''(1) = 0.$ The proportional damping makes time coordinates $\alpha_i(t)$ independent. Thus, if the damping is sub-critical the phase shift of each eigen-form is constant over the whole definition interval.

Adopting assumption of a small rotation φ, an approximate Lagrangian system for components $\zeta(t), \varphi(t)$ and $\alpha_i(t)$ can be obtained after applying the Hamilton's principle:

$$\ddot{\zeta}(t) - \frac{1}{4}\kappa_0 \frac{d^2}{dt^2}\left(\varphi^2(t)\right) - \kappa_0 \sum_{i=1}^{n} \left[\frac{\mathrm{d}}{\mathrm{d}t}\left(\varphi(t)\dot{\alpha}_i(t)\right)\theta_{0,i}\right] + \omega_0^2\left[\zeta(t) - \zeta_0(t) + \eta_c(\dot{\zeta}(t) - \dot{\zeta}_0(t))\right] = 0, \tag{4a}$$

$$\ddot{\varphi}(t) - \frac{1}{2}\kappa_1 \ddot{\zeta}(t)\varphi(t) + \kappa_1 \sum_{i=1}^{n}\left[\ddot{\alpha}_i(t)\theta_{1,i} + \left(\dot{\zeta}(t)\dot{\alpha}_i(t) - \omega_2^2\alpha_i(t)\right)\theta_{0,i}\right] + \omega_1^2\left[\varphi(t) + \eta_c\dot{\varphi}(t)\right] = 0 \tag{4b}$$

$$\ddot{\alpha}_i(t)\cdot\theta_{2,i} + \ddot{\varphi}(t)\cdot\theta_{1,0} - \left[\frac{\mathrm{d}}{\mathrm{d}t}\left(\dot{\zeta}(t)\varphi(t)\right) + \omega_2^2\varphi(t)\right]\cdot\theta_{0,i} + \omega_3^2\left[\alpha_i(t) + \eta_e\dot{\alpha}(t)\right]\theta_{3,i} = 0, \tag{4c}$$

where

$$\kappa_0 = \frac{m}{M+m}, \qquad \kappa_1 = \frac{m}{M\rho^2 + m/3}, \tag{5a}$$

$$\omega_0^2 = \frac{C}{M+m}, \qquad \omega_1^2 = \frac{C\rho^2}{M\rho^2 + m/3}, \qquad \omega_2^2 = \frac{g}{l}, \qquad \omega_3^2 = \frac{EI}{ml^3} \tag{5b}$$

$$\theta_{0,i} = \int_0^1 \chi_i(\xi)\mathrm{d}\xi, \quad \theta_{1,i} = \int_0^1 \xi\chi_i(\xi)\mathrm{d}\xi, \quad \theta_{2,i} = \int_0^1 \chi_i^2(\xi)\mathrm{d}\xi, \quad \theta_{3,i} = \int_0^1 (\chi_i''(\xi))^2\mathrm{d}\xi. \tag{5c}$$

The eigen-functions of Eq. (3) with respective boundary conditions have a detailed form as follows:

$$\chi_i(\xi) = (C_1\cdot\cos\lambda_i\xi + C_2\cdot\sin\lambda_i\xi + C_3\cdot\mathrm{ch}\lambda_i\xi + C_4\cdot\mathrm{sh}\lambda_i\xi,) \tag{6}$$

where the constants $C_1,\dots,C_4$ are defined as

$$C_1 = \sin\lambda_i \mathrm{sh}\lambda_i, \qquad C_2 = -\sin\lambda_i \mathrm{ch}\lambda_i - \cos\lambda_i \mathrm{sh}\lambda_i,$$
$$C_3 = -\sin\lambda_i \mathrm{sh}\lambda_i, \quad C_4 = \sin\lambda_i \mathrm{ch}\lambda_i + \cos\lambda_i \mathrm{sh}\lambda_i.$$

The coefficients $\lambda_i = 1.8751, 4.6941, 7.8548, 10.9955, ...$, are solutions of the transcendent equation:

$$\mathrm{ch}\lambda_i \cdot \cos\lambda_i + 1 = 0. \tag{7}$$

The analytical form of parameters $\theta_{j,i}$ in Eq. (5c) can be carried out. However, the expressions are complicated and do not bring any advantage compared to numerical solution.

The differential system (4) relates components $\zeta(t), \varphi(t)$ and $\alpha_i(t)$ and describes the time dependent behaviour of the structure. Although the console bending is considered linear, the components $\alpha_i(t)$ are non-linearly related to $\zeta(t), \varphi(t)$. However, the mutual link of $\alpha_i(t)$ components is not complicated because the relevant eigen-forms χ_i and their second derivatives χ_i'' in the meaning of Eq. (3) and respective boundary conditions are orthogonal. This fact follows from linearity of the bending component and proportionality of its damping.

Concerning the excitation process $\zeta_0(t)$, it will be considered as harmonic in order to investigate limits of stable semi-trivial and post-critical regimes. When transformed into the dimensionless form, it can be written:

$$y_0 = A_0 \sin\omega t \quad \Rightarrow \quad \zeta_0 = a_0 \cdot \sin\omega t\ , \quad A_0 = a_0 \cdot l \tag{8}$$

Let us assume that the stationary semi-trivial solution exists. It can be written as follows:

$$\begin{aligned} &\zeta_s = a_c \cdot \cos\omega t + a_s \cdot \sin\omega t\ , \\ &\varphi = 0\ , \\ &\alpha_i = 0 \end{aligned} \tag{9}$$

Substituting Eqs (9) into the system (4), Eqs (4b) and (4c) are satisfied identically, while Eq. (4a) using obvious modifications provides the coefficients a_c, a_s:

$$a_c = -\frac{a_0\omega_0^2}{\delta}\omega^3\eta_c\ ,\ a_s = \frac{a_0\omega_0^2}{\delta}(\omega_0^2 - \omega^2 + \omega_0^2\omega^2\eta_c^2)\ ,\ \delta = (\omega^2 - \omega_0^2)^2 + \omega_0^4\omega^2\eta_c^2 \tag{10}$$

Expression (9) together with coefficients (10) represents an approximate simple linear stationary solution of the single degree of freedom (SDOF) system, which moves in vertical direction and which is excited kinematically in the point B. The resonance curve of the response amplitude has the form:

$$R_0^2 = a_c^2 + a_s^2 = \frac{a_0^2\omega_0^4}{\delta}(1 + \omega^2\eta_c^2) \tag{11}$$

Stability of the semi-trivial solution (9) can be verified using the linear perturbation approach. To proceed, let us supplement the assumed semi-trivial formula (9) with a small harmonic perturbation in each component:

$$\zeta(t) = \zeta_s(t) + q(t)\ , \qquad q(t) = q_c(t)\cos\omega t + q_s(t)\sin\omega t\ , \tag{12a}$$

$$\varphi(t) = 0 + p(t)\ , \qquad p(t) = p_c(t)\cos\frac{1}{2}\omega t + p_s(t)\sin\frac{1}{2}\omega t\ , \tag{12b}$$

$$\alpha_i(t) = 0 + s_i(t)\ , \qquad s_i(t) = s_{c,i}(t)\cos\frac{1}{2}\omega t + s_{s,i}(t)\sin\frac{1}{2}\omega t\ . \tag{12c}$$

The perturbation amplitudes $q_c(t), q_s(t), ...$ are supposed to be small in absolute value. The argument (t) will be omitted in further text whenever possible $(\zeta, \varphi, \alpha_i, q, q_c, q_s, ...)$ etc.

Introducing expression (12a) into Eq. (4a) and taking into account that ζ_s represents the semi-trivial solution, following equation for perturbation q can be extracted:

$$\ddot{q} + \omega_0^2(q + \eta_c \dot{q}) \;=\; 0 \tag{13}$$

Eq. (13) is linear and homogeneous. If $\eta_c > 0$, its stationary solution vanish for sufficiently large t. Thus, the vertical response component ζ remains independent and stable in the neighbourhood of the semi-trivial solution ζ_s (on the level of the linear perturbation approach).

Using perturbed form of the semi-trivial solution (12) in Eqs (4b,c) and keeping only the linear terms of perturbations p, s_i and respecting that $q \equiv 0$, the following differential system can be obtained:

$$\ddot{p}(t) - \frac{1}{2}\kappa_1 \ddot{\zeta}_s(t)p(t) + \kappa_1 \sum_{i=1}^{n} \left[\ddot{s}_i(t)\theta_{1,i} + \dot{\zeta}_s(t)\dot{s}_i(t)\theta_{0,i} - \omega_2^2 s_i(t)\theta_{0,i}\right] + \omega_1^2\left(p(t) + \eta_c \dot{p}(t)\right) = 0, \tag{14a}$$

$$\ddot{s}_i(t)\theta_{2,i} + \ddot{p}(t)\theta_{1,i} - \left(\ddot{\zeta}_s(t)p(t) + \dot{\zeta}_s(t)\dot{p}(t)\right)\theta_{0,i} - \omega_2^2\theta_{0,i}p(t) + \omega_3^2\theta_{3,i}\left(s_i(t) + \eta_e \dot{s}_i(t)\right) = 0. \tag{14b}$$

The system (14) is of the Mathieu type (with parametric excitation) and its solution stability should be verified, cf. for instance (Abarbanel et al., 1990) or (Xu and Cheung, 1994).

The perturbations $p(t), s_i(t)$ in Eqs (14) will be replaced by means of their first harmonics, see Eqs (12). The number of unknown functions is doubled by this step. Thus it allows to formulate additional conditions. A common choice in the harmonic balance procedure is the following expression for the first derivatives of the general solution (12):

$$\begin{aligned}
\dot{q}(t) &= -q_c(t)\omega\sin\omega t + q_s(t)\omega\cos\omega t \\
\dot{p}(t) &= -\frac{1}{2}p_c(t)\omega\sin\frac{1}{2}\omega t + \frac{1}{2}p_s(t)\omega\cos\frac{1}{2}\omega t \\
\dot{s}_i(t) &= -\frac{1}{2}s_{c,i}(t)\omega\sin\frac{1}{2}\omega t + \frac{1}{2}s_{s,i}(t)\omega\cos\frac{1}{2}\omega t
\end{aligned} \tag{15}$$

Substituting the expressions (12) into (14), taking into account the new conditions (15) and applying the harmonic balance procedure, the following differential system of the first order can be obtained for parameters $p_s, p_c, s_{s,i}, s_{c,i}$:

$$\mathbf{M}\dot{\mathbf{u}} = \mathbf{H}\mathbf{u} \tag{16}$$

where $\mathbf{u} = (p_s, p_c, s_{s,1}, s_{c,1}, \ldots, s_{s,n}, s_{c,n})^T$ is the vector of unknown functions and the coefficient matrices $\mathbf{M}$, $\mathbf{H}$ are given as (n is a number of eigen-vectors taken into account)

$$\mathbf{M} = \omega \begin{pmatrix} \frac{1}{\kappa_1}\mathbf{J}, & \theta_{1,1}\mathbf{J}, & \theta_{1,2}\mathbf{J}, & \cdots & \theta_{1,n}\mathbf{J} \\ \theta_{1,1}\mathbf{J}, & \theta_{2,1}\mathbf{J}, & \mathbf{0}, & \cdots & \mathbf{0} \\ \theta_{1,2}\mathbf{J}, & \mathbf{0}, & \theta_{2,2}\mathbf{J}, & \mathbf{0}, & \vdots \\ \vdots & \vdots & & \ddots & \mathbf{0} \\ \theta_{1,n}\mathbf{J}, & \mathbf{0}, & \cdots & \mathbf{0}, & \theta_{2,n}\mathbf{J} \end{pmatrix}, \qquad \mathbf{H} = \frac{1}{2}\begin{pmatrix} \mathbf{P}, & \mathbf{S}_1, & \mathbf{S}_2, & \cdots & \mathbf{S}_n \\ \mathbf{S}_1, & \mathbf{D}_1, & \mathbf{0}, & \cdots & \mathbf{0} \\ \mathbf{S}_2, & \mathbf{0}, & \mathbf{D}_2, & \ddots & \vdots \\ \vdots & \vdots & \ddots & \ddots & \mathbf{0} \\ \mathbf{S}_n, & \mathbf{0}, & \cdots & \mathbf{0}, & \mathbf{D}_n \end{pmatrix} \tag{17}$$

and the sub-matrices $\mathbf{P}, \mathbf{S}_i, \mathbf{D}_i, \mathbf{J} \in \mathbb{R}^{2\times 2}$ have a form as follows:

$$\mathbf{P} = \begin{pmatrix} -\omega(\omega a_s + 2\omega_1^2\eta_c\kappa_1^{-1}), & (\omega^2-4\omega_1^2)\kappa_1^{-1} - \omega^2 a_c \\ (\omega^2-4\omega_1^2)\kappa_1^{-1} + \omega^2 a_c, & -\omega(\omega a_s - 2\omega_1^2\eta_c\kappa_1^{-1}) \end{pmatrix},$$

$$\mathbf{S}_i = \begin{pmatrix} -\omega^2 a_s\theta_{0,1}, & \theta_{1,1}\omega^2 + \left(4\omega_2^2 - \omega^2 a_c\right)\theta_{0,1} \\ \theta_{1,1}\omega^2 + \left(4\omega_2^2 + a_c\omega^2\right)\theta_{0,1}, & -\omega^2 a_s\theta_{0,1} \end{pmatrix}, \tag{18}$$

$$\mathbf{D}_i = \begin{pmatrix} -2\omega\eta_e\omega_3^2\theta_{3,i}, & \omega^2\theta_{2,i} - 4\omega_3^2\theta_{3,i} \\ \omega^2\theta_{2,i} - 4\omega_3^2\theta_{3,i}, & 2\omega\eta_e\omega_3^2\theta_{3,i} \end{pmatrix}, \qquad \mathbf{J} = \begin{pmatrix} 1, & 0 \\ 0, & -1 \end{pmatrix}.$$

As can be seen from the structure of the individual matrices in Eq. (18), the differential system is linear and its stability can be checked using usual approaches. It can be shown that the determinant of the matrix $\mathbf{M}$ for a given n and $\omega > 0$ does not change sign, and thus the matrix $\mathbf{M}$ is always regular and invertible. Consequently differential system (16) can be rewritten formally in a normal form

$$\dot{\mathbf{u}} = \mathbf{M}^{-1}\mathbf{H}\mathbf{u} \tag{19}$$

and its stability can be checked using eigenvalue analysis. As the signum of the determinant $\det(\mathbf{M})$ does not depend on system parameters, the matrix $\mathbf{H}$ can be used instead of the full matrix in Eq. (19).

The differential system Eqs (16) is meaningful only if the system response is at least nearly stationary in order to be entitled to use the harmonic balance method. Thus, the functions $p_c, p_s, s_{c,i}, s_{s,i}$, are functions of the ”slow time” and although they are dependent on time, it should pe possible to approximate them by constants at least within one period. Otherwise, the harmonic balance method is inapplicable and the system (20) becomes meaningless. In case of non-stationary or even chaotic response, see, e.g., papers (Abarbanel et al., 1990; Baker, 1995; Hatwal et al., 1983).

In case of stationary response the generalised amplitudes $\mathbf{u}$ can be considered to be constants. Thus, $\dot{\mathbf{u}} = 0$ and differential system (16) changes into an algebraic equation of dimension $(2n+2)\times(2n+2)$:

$$\mathbf{H}\mathbf{u} = \mathbf{0}. \tag{20}$$

The block character of the matrix $\mathbf{H}$ (17) allows to eliminate the sub-vectors $\mathbf{s}_i = (s_{s,i}, s_{c,i})^T$. Following system of dimension 2×2 for unknown vector $\mathbf{p} = (p_s, p_c)^T$ then can be obtained:

$$(\mathbf{P} - \sum_{i=1}^{n} \mathbf{S}_i \cdot \mathbf{D}_i^{-1} \cdot \mathbf{S}_i) \cdot \mathbf{p} = \mathbf{0} \tag{21}$$

Although expression (21) is complicated, the inversions $\mathbf{D}_i^{-1}$ exist for every i because $\det(\mathbf{D})$ is for $\eta_e > 0$ always negative. Indeed, if $\eta_e = 0$, the determinant $\det(\mathbf{D})$ vanish for

$$\omega = 4\omega_3^2 \frac{\theta_{3,i}}{\theta_{2,i}} = 4\frac{EI}{ml^3}\frac{\theta_{3,i}}{\theta_{2,i}}, \tag{22}$$

i.e. when ω relates to the ith eigen-frequency of the console ($\omega_{c,i} = \lambda_i\omega_3$). The constant ratios $\theta_{3,i}/\theta_{2,i}$ are approximately $0.0809, 0.00206, 0.00026, 0.00007, \ldots$ for $i = 1, 2, \ldots$.

Each of the both versions, (20) or compact (21), is suitable for a particular purpose. For instance the basic stability analysis can be performed employing the compact version of the system (21). The eigen-vectors $\mathbf{p}_{(j)}$ can be computed using the compact system, whereas the sub-vectors $\mathbf{s}_{i(j)}$ can be then subsequently computed by back substitution in the large version of the system (20).

A non-trivial solution $\mathbf{u}$ of the system (20) exist if and only it the determinant $\det(\mathbf{H})$ vanishes. Using the compact form Eq. (21) the determinant $\det(\mathbf{H})$ can be written as

$$\det(\mathbf{H}) = \det\left(\mathbf{P} - \sum_{i=1}^{n} \mathbf{S}_i \cdot \mathbf{D}_i^{-1} \cdot \mathbf{S}_i\right) \prod_{i=1}^{n} \det\left(\mathbf{D}_i\right) \tag{23}$$

As the individual $\det(\mathbf{D}_i)$ are non-zero, the first term in the product (23) is most significant. Its zero value governs the existence of non-trivial $\mathbf{u}$ in (20) and indicates instability of the system.

RESONANCE PROPERTIES

In order to analyse the resonance properties of the stationary solution of the basic system (4) we assume the response of the system in a form analogical to expressions (12):

$$\zeta(t) = a_c(t)\cos\omega t + a_s(t)\sin\omega t\ , \tag{24a}$$

$$\varphi(t) = p_c(t)\cos\frac{1}{2}\omega t + p_s(t)\sin\frac{1}{2}\omega t\ , \tag{24b}$$

$$\alpha_i(t) = s_{c,i}(t)\cos\frac{1}{2}\omega t + s_{s,i}(t)\sin\frac{1}{2}\omega t\ . \tag{24c}$$

Because an influence of the higher eigen-forms of the console can be expected as negligible, for sake of simplicity we will assume $n = 1$, i.e. single eigen-form is taken into account.

For the harmonic balance procedure we employ the additional conditions (15) once again. The differential system resulting from the harmonic balance procedure will be non-linear in this case. The vector of unknowns will be denoted as $\mathbf{x} = (a_s, a_c, p_s, p_c, s_{s,1}, s_{c,1})$, where the implicit dependence on t is assumed. The differential system can be symbolically written as

$$\mathbf{N}\dot{\mathbf{x}} = \mathbf{F}(\mathbf{x}) \tag{25}$$

The structure of the system matrix $\mathbf{N}$ is analogical to structure of the matrix $\mathbf{M}$ in Eq. (17), however, it comprises amplitudes p_s, p_c. Because we are interested in the stationary solution, which is characterised by $\dot{\mathbf{x}} = 0$, the detailed structure of $\mathbf{M}$ will be omitted here. The function $\mathbf{F}(\mathbf{x})$ on the right hand side of Eq. (25) reads:

$$\mathbf{F}(\mathbf{x}) =$$

$$\begin{pmatrix}
p_s\left(14a_c\omega^2 + \frac{5}{\kappa_1}(\omega^2 - 4\omega_1^2)\right) + 2p_c\left(2a_s\omega^2 + \frac{5}{\kappa_1}\eta_c\omega_1^2\omega\right) - \\
\qquad - s_{s,1}\left((4a_c\theta_{0,1} - 5\theta_{1,1})\omega^2 - 20\omega_2^2\theta_{0,1}\right) - 14a_s s_{c,1}\theta_{0,1}\omega^2 \\
p_c\left(2a_c\omega^2 - \frac{5}{\kappa_1}(\omega^2 + 4\omega_1^2)\right) + 2p_s\left(4a_s\omega^2 + \frac{5}{\kappa_1}\eta_c\omega_1^2\omega\right) + \\
\qquad + s_{c,1}\left((8a_c\theta_{0,1} - 5\theta_{1,1})\omega^2 - 20\omega_2^2\theta_{0,1}\right) + 2a_s s_{s,1}\theta_{0,1}\omega^2 \\
22p_c a_s\theta_{0,1}\omega^2 + p_s\left((32a_c\theta_{0,1} + 5\theta_{1,1})\omega^2 + 20\omega_2^2\theta_{0,1}\right) + 10\eta_e\omega_3^2 s_{c,1}\theta_{3,1}\omega + 5s_{s,1}\left(\omega^2\theta_{2,1} - 4\omega_3^2\theta_{3,1}\right) \\
14p_s a_s\theta_{0,1}\omega^2 - p_c\left((4a_c\theta_{0,1} + 5\theta_{1,1})\omega^2 + 20\omega_2^2\theta_{0,1}\right) + 10s_{s,1}\eta_e\omega_3^2\theta_{3,1}\omega - 5s_{c,1}\left(\omega^2\theta_{2,1} - 4\omega_3^2\theta_{3,1}\right) \\
\kappa_0\omega^2\left(2\theta_{0,1}\left(p_c s_{c,1} - p_s s_{s,1}\right) + p_c^2 - p_s^2\right) + 8\omega_0^2\omega\eta_c a_s + 8\left(\omega_0^2 - \omega^2\right)a_c + 8\omega_0^2\omega\eta_c\, a_0 \\
\kappa_0\omega^2\left(\theta_{0,1}(p_s s_{c,1} + p_c s_{s,1}) + p_c p_s\right) - 4\omega_0^2\omega\eta_c a_c - 4\left(\omega^2 - \omega_0^2\right)a_s - 4\omega_0^2\, a_0
\end{pmatrix} \tag{26}$$

The stationary solutions can be obtained as the solutions to the algebraic equation

$$\mathbf{F}(\mathbf{x}) = 0 \tag{27}$$

Roots of the systems (27) should be sought via appropriate numerical procedure. There will be always several real roots for a single excitation frequency ω and amplitude a_0. Among them, the semi-trivial solution (10) is always present as a simple real root.

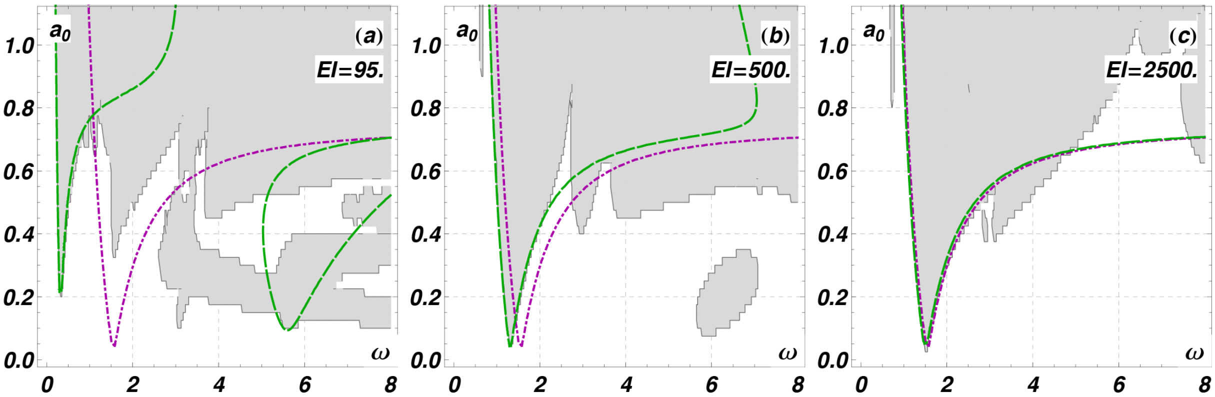

Figure 2: The stability limits in the (ω, a_0) plane of the semi-trivial solution including none (dashed green line) and one (dot-dashed magenta line) console eigen-form $(n = 0, 1)$ for varying bending stiffnesses of the console. Other system parameters: $m = 1, M = 10, C = 11, \rho = 1/5, l = 40\rho$ and dampings $\eta_c = 0.05, \eta_e = 0.05$. Greyish areas correspond to the unstable configurations.

Time coordinate has been eliminated in the Eq. (27), so the individual roots can be considered to be dependent on the excitation frequency ω. Thus, the resonance curves of the individual components of the original system can be presented as the frequency/amplitude plots of the following quantities

$$R^2 = a_c^2 + a_s^2 \;, \qquad P^2 = p_c^2 + p_s^2 \;, \qquad S_i^2 = s_{c,i}^2 + s_{s,i}^2 \tag{28}$$

where the R, P, S are amplitudes of vertical movement, angular rotation and bending of the console, respectively.

Stability of the particular solution/resonance curve should be assessed by evaluating the Jacobi determinant $\det(\partial_{\mathbf{x}}\mathbf{F})$ for particular $\mathbf{x}$. Negative value of the Jacobian indicates stable solution. The sample analysis will be presented below.

NUMERICAL EXAMPLE

In this section we show application of the described analysis. The parameters of the structure in the Figure 1 were selected artificially and do not correspond any real case. Instead, various combinations of values were applied in order to obtain typical results concerning stability of the solutions.

Performance of the stability indicator Eq. (21) is shown in Figure 2. Each plot in the figure shows the stability limits in the (ω, a_0) plane for selected bending stifnesses of the console $EI = 95, 500, 2500$ in figures (a), (b), (c), respectively. Zero trace of the determinant of the compact matrix Eq. (21) considering none or one console eigen-form is shown as a dot-dashed magenta line and dashed green line, respectively. The plots are supplemented by results of a numerical solution to the original approximate Lagrangian system (4) for $n = 3$. The greyish area shows (ω, a_0) configurations, where the response rises continuously; this violates the stability assumption and leads to failure of the structure. The correspondence between the stability limit for $n = 1$ and the numerically obtained failure is fairly good for lower excitation frequencies for all bending stifnesses. The dot-dashed magenta (case $n = 0$) is the same in every plot (it does not depend on the bending stiffness), whereas the green dashed line (case $n = 1$) approaches the undeformable case $(n = 0)$ for increasing EI. The "isola" in the plot (a) moves to higher frequencies for increasing EI and is missing from the plot (b). However, the numerical solution shows a diverging isola in case (b) for rather low excitation amplitudes. It is relevant to note that although the numerical simulation procedure considered $n = 3$ eigen-forms, contribution of the second and third eigen-form was negligible. This confirms the simplifying assumption from beginning of the preceding section.

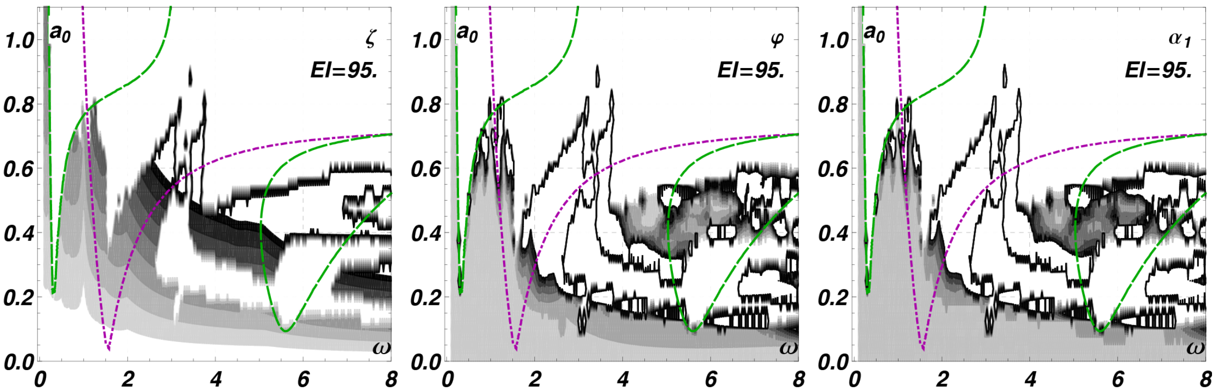

Figure 3: The numerically computed maximal amplitudes of the individual components of the response in the (ω, a_0) plane. White (empty) areas indicate the unstable configurations, levels of gray correspond to the relative maximal amplitude in the respective component. For dashed and dot-dashed lines, cf. Figure 2. Model parameters as in Figure 2, $EI = 95$.

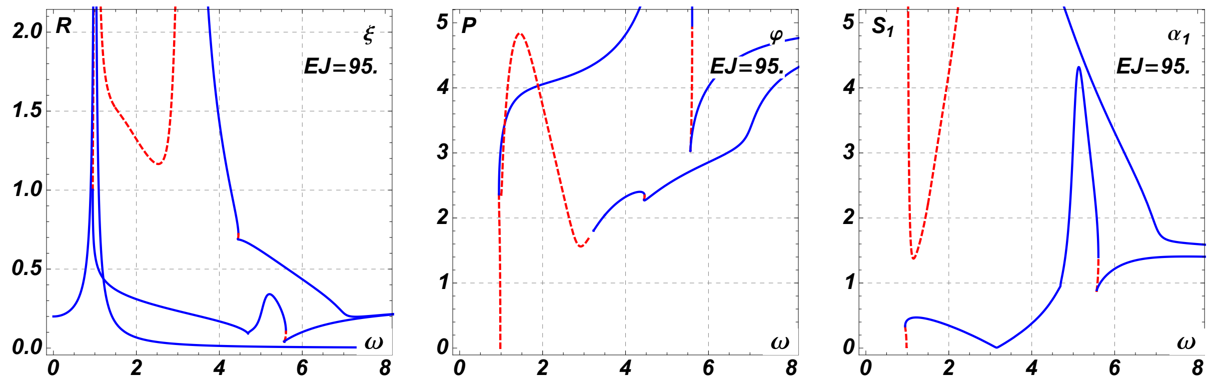

Figure 4: The resonance curves of the stationary solution in individual components of the response: blue solid lines – stable solution, red dashed lines – unstable solution. Model parameters as in Figure 3, $a_0 = 0.2$.

Figure 3 is presented as a supplement of Figure 2(a). It shows the numerically computed maximal amplitudes of the individual components of the response in the (ω, a_0) plane. On contrary to Figure2, the white (empty) areas indicate the unstable configurations, where the response cannot be reasonably determined. Levels of gray correspond to the relative maximal amplitude in the respective component. Here darker color indicate higher values of response, the black areas show the configuration, where the maximal amplitude for the particular component is reached. In this figure can be seen better than in the previous one that the lower end of the theoretical isola is well respected by the numerical results. On the other hand, stability indicators based on determinants of system matrices in Eq. (20) or (21) give evidence only on the validity of the semi-trivial solution. Their information value regarding parameters φ or α_i is very limited.

The resonance properties of the stationary solution are illustrated in Figure 4. The three plots show non-trivial solutions of the algebraic system (27) for a single excitation amplitude $a_0 = 0.2$. The semi-trivial solution is the lowest curve in the left graph (ζ), it has no corresponding lines in the other plots. The other roots have all three (resp. six) components non-trivial. Stability of the individual traces has been checked via evaluation of the Jacobian. The stable solutions are shown as solid blue curves in Figure 4 and the unstable solutions are indicated as dashed red lines. Care should be taken when a multiple solution is found. It can have stable and unstable branches simultaneously. This type of solution usually cannot be reached in practice.

CONCLUSIONS

The auto-parametric resonance effect, which affects the easily deformable tall structures like chimneys, towers or masts, is studied in detail. If the amplitude of a vertical excitation in a structure foundation exceeds a certain limit, a vertical response component loses stability and dominant horizontal response component arises. This post-critical regime (auto-parametric resonance) follows from the non-linear interaction of vertical and horizontal response components and can lead to a failure of the structure. Although the purely vertical seismic excitation at a large scale is mostly an hypothesis, some particular cases at a lower scale have been repeatedly reported being caused due to local site conditions.

Hamiltonian functional is formulated and subsequently respective Lagrangian governing system is set up. Differential system shows that horizontal and vertical response components are independent on the linear level. Their interaction takes place due to non-linear terms in post-critical regime only. The semi-trivial solution is identified and its stability is studied using the harmonic balance procedure. Performance of the determinant-based criterion is compared to the numerical simulation. It is found that especially in the area close to the first eigen-frequency of the structure is the criterion acceptable.

The individual resonance curves, which determine the stationary solutions in the (ω, a_0) (excitation frequency vs. amplitude) plane, are determined via solution to the non-linear algebraic equation. Their stability or instability is checked using the corresponding Jacobian.

The general methods combining analytical and numerical approaches were developed and used. Their applicability and shortcomings are commented. A few hints for engineering applications in a design practice are given.

ACKNOWLEDGEMENT

The kind support of the Czech Science Foundation project GA CR 13-34405J and of the RVO 68378297 institutional support are gratefully acknowledged.

REFERENCES

Abarbanel HDI, Brown R, Kadtke JB (1990) ”Prediction in chaotic nonlinear systems: Methods for time series with broadband Fourier spectra”, *Physical Rewiews A*, 41, 1782-1807.

Ambraseys N, Douglas J (2000) ”Reappraisal of the effect of vertical ground motions on response”, ESEE Report No. 00-4. Imperial College, Civil and Environmental Engineering Dept., London.

Bajaj AK, Chang SI, Johnson JM (1994) ”Amplitude modulated dynamics of a resonantly excited autoparametric two degree of freedom system”, *Nonlinear dynamics*, 5, 433–457.

Baker GL (1995) ”Control of the chaotic driven pendulum”, *American Journal of Physics*, 63, 832–838.

Benettin G, Galgani L, Giorgilli A, Strelcyn M (1980) ”Lyapunov characteristic exponents for smooth dynamical systems and Hamiltonian systems: A method for computing all of them. Part 2, Numerical application”, *Meccanica*, 15, 9–21.

Broderick BM, A.S. Elnashai AS(1995) ”Analysis of the failure of Interstate 10 freeway ramp during the Northridge earthquake of 17 January 1994”, *Earthquake Eng Struct Dyn*, 24, 189–208, 1995.

Carydis P, Castiglioni C, Lekkas E, Kostaki I, Lebesis N, Drei A (2012) ”The Emilia Romagna, May 2012 earthquake sequence. The influence of the vertical earthquake component and related geoscientific and engineering aspects”, *Ingegneria Sismica*, 29,2–3, 31–58 , 2012.

Elnashai AS, Papazoglou AJ (1996) Analytical and field evidence of the damaging effect of vertical earthquake ground motion, *Earthquake Eng Struct Dyn*, 25, 1109–1137.

Hatwal H, Mallik AK, Ghosh A (1983) ”Forced nonlinear oscillations of an autoparametric system”, *ASME Jour. Applied Mechanics*, 50, 657–662.

Náprstek J, Fischer C (2008) ”Non-linear auto-parametric stability loss of a slender structure due to random non-stationary seismic excitation”, in: *Proc. 14th Word Conference on Earthquake Engineering.* Chinese Assoc. Earthq. Eng., Beijing, pgs 8.

Náprstek J, Fischer C (2009) ”Auto-parametric semi-trivial and post-critical response of a spherical pendulum damper”, *Computers & Structures*, 87, 19–20, pp. 1204–1215.

Náprstek J, Fischer C (2011) ”Auto-parametric Stability Loss and Post-critical Behavior of a Three Degrees of Freedom System”, *Computational Methods in Stochastic Dynamics*, M. Papadrakakis et al. (Editors), Springer, Chapter 14 , 267–289.

Náprstek J, Fischer C (2012) ”Dynamic Stability of a Non-linear Continuous System Subjected to Vertical Seismic Excitation”, in *Proceedings of the Eleventh International Conference on Computational Structures Technology*, B.H.V. Topping, (Editor), Civil-Comp Press, Stirlingshire, United Kingdom, paper 179. doi:10.4203/ccp.99.179

Tondl A, Ruijgrok T, Verhulst F, Nabergoj R (2000) ”Autoparametric Resonance in Mechanical Systems”, Cambridge University Press, Cambridge.

Xu Z, Cheung YK (1994) ”Averaging method using generalized harmonic functions for strongly non-linear oscillators”, *Journal of Sound and Vibration*, vol. 174, 4, 563–576.